Molecular orientation in flat plates of liquid-crystalline polymer using low-cost reflectance Fourier-transform infra-red microscopy

J. A. J. Jansen* and F. N. Paridaans
Philips Competence Centre Plastics BV, PO Box 218, 5600 MD Eindhoven, The Netherlands

and I. E. J. Heynderickx
Philips Research Laboratories, Eindhoven, The Netherlands
(Received 4 March 1993; revised 16 November 1993)

The direction of the averaged molecular orientation as well as the order parameter in injection-moulded flat plates of liquid-crystalline polymer (Vectra A950, A530 and A130) were investigated by infra-red dichroism. The measurements were performed with a low-cost Fourier-transform infra-red reflectance microscope. Lateral and depth profiles, inclusive of three-dimensional imaging, of the molecular orientation were measured as a function of thickness of the flat plate and injection speed.

(Keywords: liquid-crystalline polymer; reflectance *FT*i.r. microscopy; molecular orientation)

INTRODUCTION

Injection moulding of polymers induces orientation of the macromolecular chains in the final products, and this greatly affects their end-use properties. For example, the injection moulding of liquid-crystalline polymer (LCP) results in products with markedly anisotropic mechanical and thermal properties[1,2]. In addition to measurement of the anistropy in macroscopic properties, there are a number of analytical techniques available to quantify the amount of molecular ordering. X-ray diffraction measurements are frequently used to determine an estimate for the width of the molecular distribution function[3,4]. Infra-red (i.r.) spectroscopy has also been shown to provide a useful tool for the investigation of orientation[5,6]. With i.r., orientation of a molecular group is characterized by the dichroic ratio R, which is the ratio of the intensities of the absorption band of a characteristic group measured for parallel ($A_{\parallel}$) and perpendicular ($A_{\perp}$) polarization of radiation with respect to the direction of orientation[7], namely:

$$R = A_{\parallel}/A_{\perp} \tag{1}$$

As will be shown later, the dichroic ratio is related to the order parameter, which, in the case of uniaxially oriented systems, can be understood as follows. In a defined x–y plane a single molecule is represented by its principal molecular axis, as shown in *Figure 1*. The direction of the molecular alignment is characterized by the director, which is taken to be parallel to the y axis of the x–y plane, e.g. the polymer flow direction. As shown in *Figure 1*, the angle between the principal molecular axis and the director is indicated by θ.

From X-ray diffraction experiments the order parameter S has been defined by Hermans[8] as:

$$S = 0.5[3\,\overline{\cos^2(\theta)} - 1] \tag{2}$$

The notation $\overline{\cos^2(\theta)}$ indicates the average of the square of the cosine of the angle between the principal molecular axis and the director. When the direction of the molecular alignment is unknown, we can use a kind of effective order parameter based on the angle ϕ between the director and

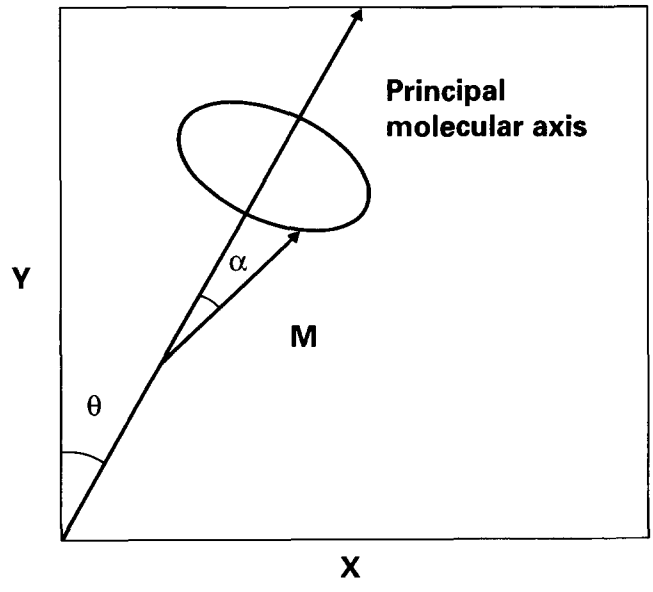

Figure 1 Definition of the angles used to specify the principal molecular axis and the dipole moment M with respect to a defined x–y plane

* To whom correspondence should be addressed

0032-3861/94/14/2970–07

an arbitrary axis in the plane of the sample. In this definition the effective order parameter S varies between -0.5 and 1, and the following values have special meanings:

$S=1$	complete order parallel to the y axis
$S=0$	complete disorder
$S=-0.5$	complete order perpendicular to the y axis

In the particular case where the director lies along the y axis, the effective order parameter equals the order parameter and varies between 1 (complete order) and 0 (random order). In this paper only the term 'order parameter' is used, which is in fact the effective order parameter because the direction of the molecular alignment is unknown.

Maier and Saupe[9] derived a relation between the order parameter and the dichroic ratio of the absorption band of a characteristic group with a dipole moment M at an angle α with respect to the principal molecular axis, so that:

$$\frac{R-1}{R+2}=0.5S[3\cos^2(\alpha)-1] \quad (3)$$

In the derivation of equation (3), Maier and Saupe assumed that the molecules are cylindrically symmetric. For deviations from this cylindrical symmetry, other relations have been derived in the literature[10–13].

For a dipole moment parallel to the principal molecular axis of the molecule, i.e. $\alpha=0$, equation (3) is simplified to:

$$\frac{R-1}{R+2}=S \quad (4)$$

Using equation (3) or (4), the order parameter can be obtained simply from i.r. dichroic measurements. These measurements may be performed both in transmission and reflection using an infra-red polarizer[14,15]. The transmission method requires a finite thickness of the sample of the order of 10 μm. The reflection method is based on attenuated total reflection (a.t.r.) spectroscopy, requiring a close optical contact between the sample and an optical crystal with a high refractive index. In this reflection mode there are no restrictions on the thickness of the sample, but an extremely flat sample area of the order of 10 mm^2 is required. These are serious limitations to the investigation of molecular orientation in complex-shaped polymeric products. Pirnia and Sung[16] have used a.t.r. to determine 3D molecular ordering profiles in injection-moulded thermotropic LCP samples.

In the present investigation, reflection measurements were performed using the low-cost reflectance *FT*i.r. microscope with diffuse reflectance optics without restrictions on shape and thickness of the measured products[17–20]. Owing to differences in reflectivity of parallel- and perpendicular-polarized light on polymers in the microscope, i.r. dichroism can be measured without using a polarizer, simply by rotating the oriented sample through 90°. Nevertheless, several experiments were performed including a polarizer to obtain improved quantitative analyses.

In polymeric products the direction of the mean molecular orientation is often unknown. By making an angular scan of i.r. spectra one finds the projection of this direction with respect to the measuring plane at the angular position where S of equation (3) or (4) attains its maximum value. The location of the director in the third dimension is determined by making an angular scan in a second plane, perpendicular to the first one.

With the microscope, lateral profiles of the molecular orientation of polymeric products can be measured by scanning the surface. Depth profiling of the molecular orientation is possible by removing layers of defined thickness before the i.r. measurements.

The results described in this paper are restricted to determining the influence of injection-moulding parameters on the resulting molecular ordering profiles in thermotropic LCP samples.

EXPERIMENTAL

Infra-red spectra were obtained with an *FT*i.r. spectrometer (Philips PU 9800) equipped with a standard deuterated triglycine sulfate (DTGS) detector at room temperature. The infra-red beam was less than 10% polarized. The low-cost *FT*i.r. reflectance microscope was used, based on a diffuse-reflectance accessory (Spectra-Tech Collector). *Figure 2* shows the optical configuration. The samples were positioned in the focal point of the microscope for maximum reflection with the aid of the x–y–z stage, adjustable in steps of 10 μm, and viewed with the monocular. The spot size of the i.r. radiation was varied from 0.3 to 3 mm with the diaphragm. The i.r. reflection spectra were ratioed against the background of an aluminium mirror. Because of the specular-reflectance nature of the technique, the i.r. bands were distorted, resulting in a first-derivative-like appearance. These spectra can be converted via a Kramers–Kronig algorithm to absorption spectra. However, Kramers and Kronig used some assumptions that are not valid for all types of samples. Therefore we prefer mathematical differentiation of the specular-reflectance spectra, which results in characteristic second-derivative-like spectra suitable for interpretation[17].

A polarizer (Specac KRS-5) was used for a number of experiments. For the depth-profiling experiments, layers of a given thickness were removed from the polymeric samples with an ultra-mill (Reichert-Jung model K). After each milling step the resulting sample thickness was measured with microcallipers.

The polymeric samples studied in this paper were standard injection-moulded flat plates[21] of LCP. The LCP was a copolymer of *p*-hydroxybenzoic acid and

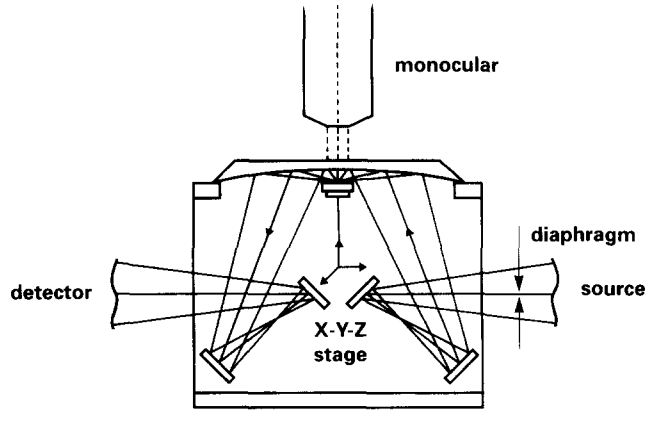

Figure 2 Optical configuration of the low-cost reflectance *FT*i.r. microscope

6-hydroxy-2-naphthoic acid (Hoechst-Celanese Vectra). We investigated not only the pure-grade Vectra A950 but also the 30% talc-filled Vectra A530 and the 30% glass-fibre-filled Vectra A130. *Figure 3* shows schematically the dimensions of the flat plate in the defined x–y plane of *Figure 1* and the locations where the i.r. dichroic measurements were performed. The flat plates were produced at two injection speeds of 10 and 1 cm s^{-1}, two thicknesses of 2 and 0.5 mm, a mass temperature of 285°C and a mould temperature of 110°C. Pieces, with maximum dimensions of 30×30 mm^2, were cut from the test samples for the i.r. measurements. During the milling operations the samples were glued onto an aluminium block. Two spectra were recorded for each measurement, with the polymer flow direction parallel and perpendicular, respectively, to the plane of incidence of the i.r. radiation, by rotating the sample through 90°. In principle, the light collected from the sample has specular-reflectance (from the front surface), transflectance (from the rear surface) and diffuse-reflectance (from the surface roughness) components. The transflectance component of our LCP specimens, i.e. transmission of two times the thickness of the specimen, was measured and found to be zero in the wavelength regions of the interesting absorption bands. No diffuse reflected components have been detected by Dr E. H. Korte with the aid of a special reflectance accessory[13]. By milling the specimens in different directions, the influence of milling on the specular-reflectance spectra and thus on the molecular orientation was negligible.

Especially for the determination of the molecular orientation distribution in three dimensions, small samples were cut from the bulk of the LCP plates. These samples were used in *FT*i.r. as well as wide-angle X-ray diffraction (WAXS) experiments. The WAXS measurements were performed by recording the Ni-filtered Cu Kα radiation (Philips PW 1830). The angular intensity distribution was analysed with an optical densitometer to calculate the order parameter using the Vainstein relation[22].

RESULTS AND DISCUSSION

Analysis of spectra

Figure 4 shows the differentiated i.r. spectra of an injection-moulded LCP flat plate, recorded at the surface at point A in the x and y directions as indicated in *Figure 3*, without the use of a polarizer. Note that the intensity of a number of bands depends on the direction of the polymer flow with respect to the i.r. radiation. This phenomenon can be explained by studying the external reflections of parallel- ($R_\parallel$) and perpendicular- ($R_\perp$) polarized i.r. radiation[19,20]. At a surface with a refractive index of 1.5 and an angle of incidence of the radiation of about 60° — the Brewster angle — $R_\parallel$ becomes zero and only $R_\perp$ is reflected. In the optical configuration of *Figure 2*, the unpolarized i.r. beam is focused on the sample with an almost equal amount of $R_\parallel$ and $R_\perp$. However, the i.r. beam has a conical distribution with an angle of incidence of the cone on the sample of about $60° \pm 10°$. Since the refractive index for polymers is about 1.5, mainly $R_\perp$ is reflected while $R_\parallel$ is extinguished at these angles. Because the refractive index is not exactly 1.5 and the angle of incidence is not exactly the Brewster angle, a polarizer was used in this investigation to obtain perfect perpendicular-polarized radiation. In practice, the use of the polarizer had only minor effects on the quantitative results.

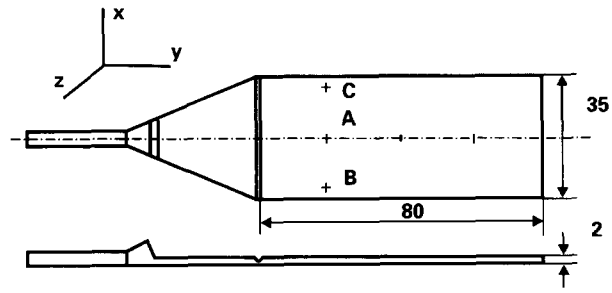

Figure 3 Schematic representation of an injection-moulded liquid-crystalline polymer flat plate in a defined x–y–z space with dimensions given in millimetres

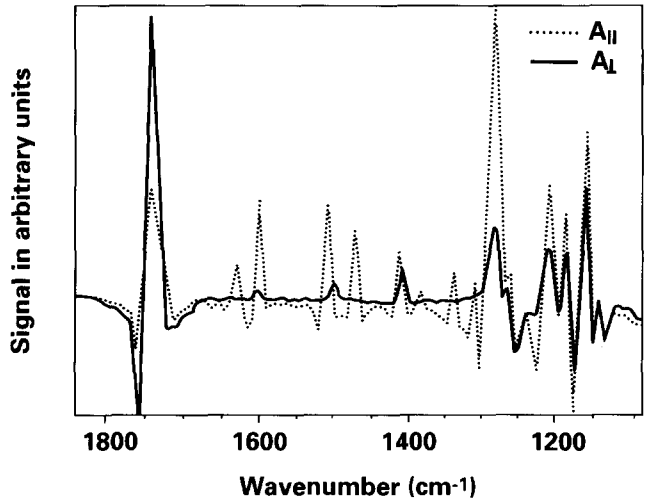

Figure 4 Differentiated i.r. reflectance spectra of the surface of an injection-moulded liquid-crystalline polymer flat plate with i.r. radiation parallel and perpendicular, respectively, to the polymer flow direction

The intensities of the absorption band of a characteristic group measured with light polarized parallel ($A_\parallel$) and perpendicular ($A_\perp$) with respect to the y axis of the defined x–y plane of *Figure 1* have been defined by Samuels as follows[23]:

$$A_\parallel = C[S\cos^2(\phi+\alpha)+(1-S)/3] \quad (5)$$

and

$$A_\perp = C[(S/2)\sin^2(\phi+\alpha)+(1-S)/3] \quad (6)$$

with ϕ the angle between the director and the y axis and C a constant proportional to the square of the transition moment of the characteristic group and the electric vector of radiation.

As already stated, the dichroic measurements were performed with perpendicular-polarized radiation. This means that the band intensity $A_\perp$ was measured with the polymer flow direction parallel to the i.r. radiation. However, by rotating the sample through, 90°, $A_\parallel^*$ was measured. $A_\parallel^*$ could be derived from equation (6), namely:

$$A_\parallel^* = C[(S/2)\sin^2(\phi+\alpha+90)+(1-S)/3]$$

i.e.

$$A_\parallel^* = C[(S/2)\cos^2(\phi+\alpha)+(1-S)/3] \quad (7)$$

Equation (7) is not equal to equation (5) and thus $A_\parallel^* \neq A_\parallel$.

The calculated dichroic ratio R^* and order parameter S^* are then defined as:

$$R^* = A_{\parallel}^*/A_{\perp} \tag{8}$$

and

$$S^* = \frac{R^* - 1}{R^* + 2} \tag{9}$$

This means that the order parameter S cannot be estimated by measuring two reflectance spectra at two sample positions, relatively 90° rotated. Fortunately, in a number of special cases the latter can be derived simply from S^*. In the case that the mean molecular orientation is at an angle α with respect to the y axis of the x–y plane in *Figure 1*, $A_{\perp}$ is measured at $(\phi+\alpha)=0°$ and $A_{\parallel}^*$ at $(\phi+\alpha+90)=90°$. From equations (5) to (9) the following relation between S and S^* can then be derived:

$$S = \frac{2S^*}{1+S^*} \tag{10}$$

In the first instance R^* and S^* are determined without knowledge of the angle θ. The angle θ is related to the maximum value of S^* while scanning the angular position of the sample. If the angle θ is known, the order parameter S can be calculated using equation (10).

In *Figure 4* the bands between 1650 and 1400 cm^{-1} are apparently a consequence of parallel orientation of the transition moment of the C=C vibrations of the aromatic ring to the molecular long axis. On the other hand, the band at 1740 cm^{-1} can be interpreted in terms of perpendicular orientation of the transition moment of the C=O stretching vibration to the molecular long axis.

Depth profiling

At the surface of the flat plates, we expect molecular orientation in the flow direction depending on the moulding conditions. A gradient of the molecular orientation from the surface to the centre of the plate is also expected[16,24–26]. Depth profiling was performed by removing defined layers with the aid of an ultra-mill. At a resolution of 8 cm^{-1} and a spot size of 1 mm^2, 250 scans were co-added and a polarizer was used. The dichroic ratios and the order parameters of the C=C vibration of the aromatic ring at 1600 cm^{-1} were calculated. *Figure 5* shows the depth profiles of the order parameter of the Vectra A950 plates with a thickness of 2 mm at point A of *Figure 3* with an injection speed of 10 and 1 cm s^{-1}, respectively, measured with respect to the flow direction. It can be seen that the profiles are very different. A common feature is the maximum at the surface and the local maximum between 100 and 200 μm. These maxima are identical with maxima obtained with general-purpose polymers such as polystyrene[21,27]. For these polymers the maximum at the surface is attributed to the fountain flow, occurring in the flow front during mould filling in which planar elongation is taking place. The local maximum is due to shear flow along a solidified layer at the cavity wall during mould filling. A similar explanation may hold for the LCP. It is remarkable that, at an injection speed of 10 cm s^{-1}, the order parameter is even negative in the core. This means that the direction of the molecular orientation has been reversed with respect to the flow direction.

The direction of the mean molecular orientation was determined at different points of the depth profiles by measuring spectra at different angles ϕ with respect to the flow direction. Spectra were measured at 4 times 2 angles (0 and 90, 22.5 and 112.5, 45 and 135, 67.5 and 157.5°, respectively), differentiated and S^* determined on the basis of the 1600 cm^{-1} band. *Figure 6* shows the results for the surface and the core of a sample injection

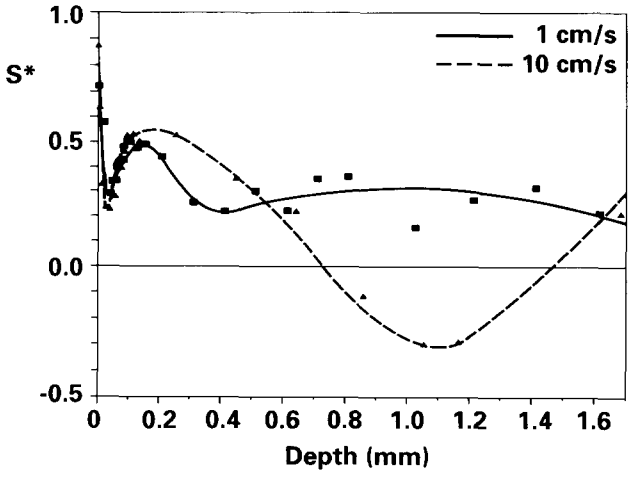

Figure 5 Depth profiles of the order parameter S^* of Vectra A950 flat plates with a thickness of 2 mm at point A as indicated in *Figure 3*, with an injection speed of 10 and 1 cm s^{-1}

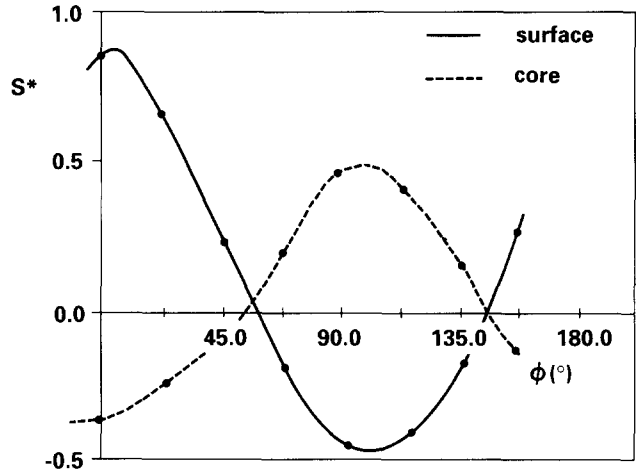

Figure 6 Order parameters S^* at the surface and in the core of the flat plate of *Figure 5* with an injection speed of 10 cm s^{-1} as a function of the measuring angle ϕ with respect to the polymer flow direction

Table 1 Direction and magnitude of the order parameter in injection-moulded Vectra A950 flat plates with a thickness of 2 mm as a function of injection speed at various depths at location A in *Figure 3*

	Direction and magnitude of order parameter			
	10 cm s^{-1}		1 cm s^{-1}	
Depth (μm)	θ (deg)	S	θ (deg)	S
0	6	0.94	5	0.92
35	6	0.36	9	0.55
60	13	0.66	−1	0.47
170	6	0.65	12	0.42
500	8	0.54	6	0.40
750	86	0.50	8	0.52
1000	97	0.61	−1	0.26

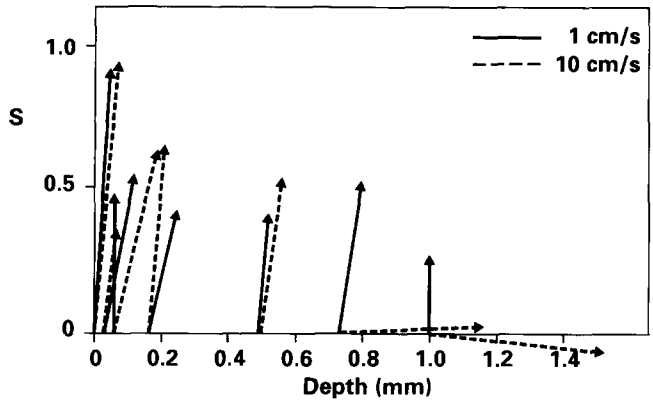

Figure 7 Vector presentation of the depth profiles of the molecular orientation at point A as indicated in *Figure 3* of Vectra A950 flat plates with a thickness of 2 mm and an injection speed of 10 and 1 cm s^{-1}

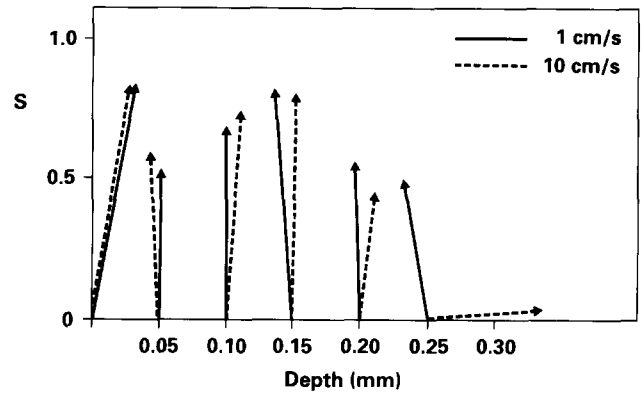

Figure 8 Vector presentation of the depth profiles of the molecular orientation at point A as indicated in *Figure 3* of Vectra A950 flat plates with a thickness of 0.5 mm and an injection speed of 10 and 1 cm s^{-1}

Table 2 Direction and magnitude of the order parameter in injection-moulded Vectra A950 flat plates with a thickness of 0.5 mm as a function of injection speed at various depths at location A in *Figure 3*

	Direction and magnitude of order parameter			
	10 cm s^{-1}		1 cm s^{-1}	
Depth (μm)	θ (deg)	S	θ (deg)	S
0	10	0.86	10	0.86
50	−2	0.60	1	0.52
100	3	0.73	0	0.68
150	1	0.80	−3	0.81
200	5	0.45	−2	0.55
250	86	0.40	−10	0.50

Table 3 Direction and magnitude of the order parameter in injection-moulded Vectra A530 flat plates with a thickness of 2 mm as a function of injection speed at various depths at location A in *Figure 3*

	Direction and magnitude of order parameter			
	10 cm s^{-1}		1 cm s^{-1}	
Depth (μm)	θ (deg)	S	θ (deg)	S
0	9	0.89	7	0.87
30	−10	0.23	7	0.39
150	−4	0.28	−10	0.11
500	5	0.34	–	–
1000	97	0.65	5	0.43

moulded at a speed of 10 cm s^{-1}. To estimate the direction of the molecular orientation a parabolic function was fitted through three points near the top of the functional behaviour of S^*. The angle ϕ at which this parabolic function reaches a maximum represents the angle θ of the principal molecular axis with respect to the flow direction, which in this case was 6° for the surface and 97° for the core, respectively. The maximum itself represents the order parameter S^*. The order parameter S was calculated using equation (10) and found to be 0.94 and 0.61, respectively. *Table 1* presents the calculated direction and magnitude of the order parameter of the Vectra A950 flat plates with a thickness of 2 mm and an injection speed of 10 and 1 cm s^{-1}, respectively, at various depths at point A as indicated in *Figure 3*. *Figure 7* is a vector presentation of the results in *Table 1*.

For the Vectra A950 flat plate with an injection speed of 10 cm s^{-1} the direction of the mean molecular orientation in the core changes between 500 and 750 μm over an angle of 90°. For the plate with an injection speed of 1 cm s^{-1} the director remains aligned along the flow direction.

Table 2 and *Figure 8* present similar depth profiles of Vectra A950 flat plates with a thickness of 0.5 mm and an injection speed of 10 and 1 cm s^{-1}, respectively, at point A of *Figure 3*. In the case of the plates with a thickness of 2 mm, the skin-to-core thickness ratio is higher for these plates, resulting in only a thin layer with molecular orientation perpendicular to the flow in the core for an injection speed of 10 cm s^{-1}.

Table 4 Direction and magnitude of the order parameter in injection-moulded Vectra A130 flat plates with a thickness of 2 mm as a function of injection speed at various depths at location A in *Figure 3*

	Direction and magnitude of order parameter			
	10 cm s^{-1}		1 cm s^{-1}	
Depth (μm)	θ (deg)	S	θ (deg)	S
0	0	0.62	0	0.67
30	5	0.04	–	–
150	−5	0.33	–	–
500	5	0.57	–	–
1000	97	0.66	5	0.38

Tables 3 and *4* show the results of flat plates with a thickness of 2 mm of Vectra A530 (talc-filled) and Vectra A130 (glass-fibre-filled), respectively. Here we also see profiles similar to those for Vectra A950 (unfilled), with a change through 90° of the direction of the molecular orientation in the core in relation to the polymer flow at an injection speed of 10 cm s^{-1}.

Figure 9 shows the results for Vectra A950, A530 and A130 flat plates with a thickness of 2 mm and an injection speed of 10 cm s^{-1} in a vector presentation. There is a tendency towards reduced molecular ordering due to the addition of a filler.

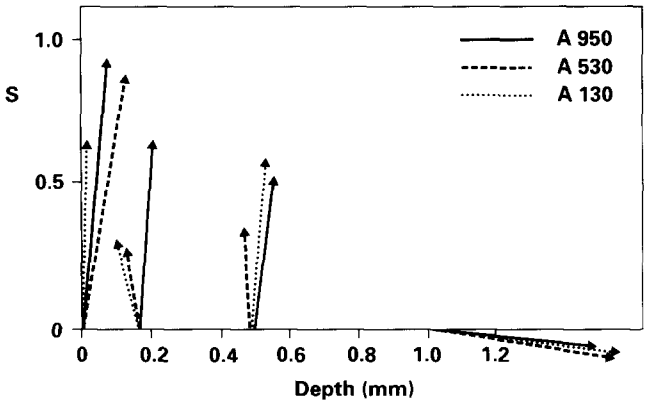

Figure 9 Vector presentation of the depth profiles of the molecular orientation at point A as indicated in *Figure 3* of Vectra A950, A530 and A130 flat plates with a thickness of 2 mm and an injection speed of 10 cm s^{-1}

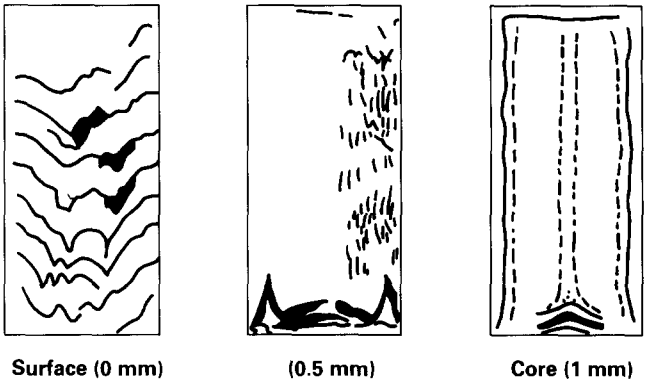

Figure 10 Irregular domains in a Vectra A950 flat plate with a thickness of 2 mm and an injection speed of 1 cm s^{-1} at different depths

Lateral profiling and 3D imaging

As shown in *Figure 10*, irregular domains were observed visually after removing layers for flat plates with a thickness of 2 mm and an injection speed of 1 cm s^{-1}. At locations A, B and C of *Figure 3* light bands of about 2 mm in width were observed in the flow direction in the core, at a depth of 1000 μm. A lateral-orientation profile was performed for the Vectra A950 flat plate in the core from A to B in steps of 1 mm. The results are presented in *Figure 11*. The molecular orientation is clearly disturbed at the locations of the observed bands. Until now, however, no explanation has been found for light and dark bands occurring in injection-moulded samples, or for their relation with molecular ordering.

The i.r. dichroic measurement only provides information about the projection of the orientation of a characteristic molecular group in a defined x–y plane. To estimate the mean molecular orientation in a defined x–y–z space at point A of *Figure 3*, small parts were milled out of the core of Vectra A950 flat plates with a thickness of 2 mm and an injection speed of 1 and 10 cm s^{-1}, respectively. The direction and magnitude of the order parameter were investigated in the x–y, x–z and y–z planes, respectively. These 3D imaging results are given in *Table 5* and schematically viewed in *Figure 12*, as it was perfectly oriented. These results demonstrate that the principal molecular axis comes out of the plane of the sample at an angle of about 10° or smaller.

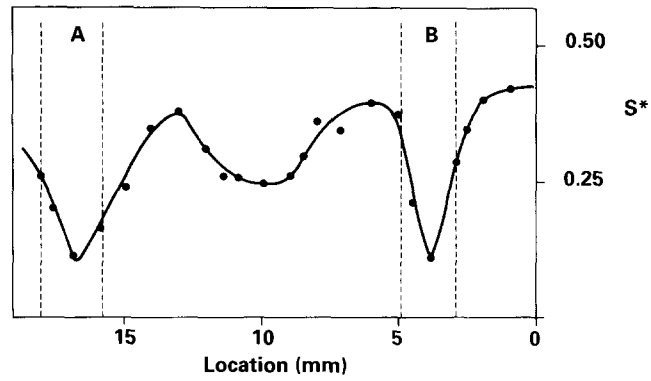

Figure 11 Lateral profile of the order paramerer S^* in the core of a Vectra A950 flat plate with a thickness of 2 mm and an injection speed of 1 cm s^{-1} from point A to B as indicated in *Figure 3*

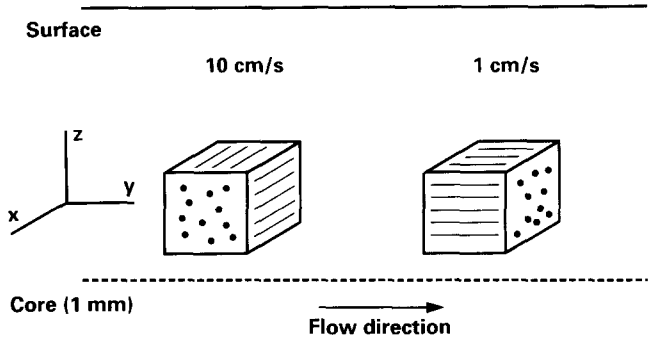

Figure 12 Three-dimensional imaging of the molecular orientation in the core at point A as indicated in *Figure 3* of Vectra A950 flat plates with a thickness of 2 mm and an injection speed of 10 and 1 cm s^{-1}

Table 5 Direction and magnitude of the order parameter in injection-moulded Vectra A950 flat plates with a thickness of 2 mm as a function of injection speed measured by i.r. with respect to different planes in the core at location A in *Figure 3*

	Direction and magnitude of order parameter			
	10 cm s^{-1}		1 cm s^{-1}	
Plane	θ (deg)	S	θ (deg)	S
x–y	95	0.60	10	0.40
x–z	5[a]	0.50	0[a]	0.20
y–z	0	0.30	10	0.40

[a] With respect to x axis

We compared the i.r. results with data obtained by WAXS experiments on the same 3D imaging samples. Analysis of the diffraction patterns also provides the order parameter as well as the angle between the director and the long axis of the sample, which was parallel to the main axes of the frame of *Figure 3*. The resulting values for the molecular-orientation distribution projected on the three principal planes in the frame of the sample are summarized in *Table 6*. The i.r. and WAXS data exhibit the same tendency. The differences can be explained by variations of the molecular orientation across the sample thickness.

Meanwhile, we have demonstrated that the i.r. dichroic measurements are in good agreement with tendencies found in mechanical properties, anisotropic

Table 6 Direction and magnitude of the order parameter in injection-moulded Vectra A950 flat plates with a thickness of 2 mm as a function of injection speed measured by WAXS with respect to different planes in the core at location A in *Figure 3*

	Direction and magnitude of order parameter			
	$10\ cm\ s^{-1}$		$1\ cm\ s^{-1}$	
Plane	θ (deg)	S	θ (deg)	S
x–y	96	0.34	6	0.37
x–z	3[a]	0.30	0[a]	0.20
y–z	5	0.40	7	0.60

[a] With respect to x axis

heat conduction and X-ray diffraction experiments, which have been published in a previous paper[28].

CONCLUSIONS

With the aid of Fourier-transform infra-red spectroscopy using the low-cost *FT*i.r. reflectance microscope, lateral and depth profiles, including 3D imaging, of the molecular orientation of LCP flat plates can be readily obtained. In addition to the order parameter (i.e. the degree of orientation) the direction of the mean molecular orientation is obtained as well. An advantage compared with i.r. transmission and internal reflection techniques is that there are hardly any restrictions on the shape and thickness of the samples.

The results for Vectra A950, A530 and A130 flat plates are comparable. The injection speed influences the direction of the molecular orientation in the core. The filler has no influence on the direction of the molecular orientation, but only on its magnitude. For plates with a thickness of 0.5 mm, the skin-to-core thickness ratio is higher than for those with a thickness of 2 mm.

REFERENCES

1 Ophir, Z. and Ide, Y. *Polym. Eng. Sci.* 1983, **23**, 792
2 Chivers, R. A. and Moore, D. R. *Polymer* 1991, **32**, 2190
3 Mitchell, G. R. and Windle, H. A. *Polymer* 1983, **24**, 1513
4 Blundell, D. J., Chivers, R. A., Curson, A. D., Lore, J. C. and MacDonald, W. A. *Polymer* 1988, **29**, 1459
5 Ward, I. M. 'Structure and Properties of Oriented Polymers', Applied Science, London, 1975
6 Jasse, B. 'Developments in Polymer Characterisation–4' (Ed. J. W. Dawkins), Applied Science, London, 1983, p. 91
7 Rabek, J. F. 'Experimental Methods in Polymer Chemistry', Wiley, New York, 1980, p. 582
8 Hermans, P. H. 'Contributions to the Physics of Cellulosic Fibres', Elsevier, Amsterdam, 1946, p. 133
9 Saupe, A. and Maier, W. *Z. Naturforsch. (a)* 1961, **16**, 816
10 Alben, R., McColl, J. R. and Shih, C. S. *Solid State Commun.* 1972, **11**, 1081
11 Straley, J. P. *Phys. Rev. (A)* 1974, **10**, 1881
12 Luckhurst, G. R., Zannoni, C., Nordio, P. L. and Segre, U. *Mol. Phys.* 1975, **30**, 1345
13 Korte, E. H. *Mol. Cryst. Liq. Cryst.* 1983, **100**, 127
14 Samuels, R. J. *Polym. Eng. Sci.* 1983, **23**, 257
15 Houska, M. and Brummel, M. *Polym. Eng. Sci.* 1987, **27**, 917
16 Pirnia, A. and Sung, C. S. P. *Macromolecules* 1988, **21**, 2699
17 Jansen, J. A. J. and Haas, W. E. *Polym. Commun.* 1988, **29**, 77
18 Jansen, J. A. J., van der Maas, J. H. and Posthuma de Boer, A. *Appl. Spectrosc.* 1991, **45**, 1149
19 Jansen, J. A. J., Thesis, Utrecht, 1992
20 Jansen, J. A. J., van der Maas, J. H. and Posthuma de Boer, A. *Macromolecules* 1991, **24**, 4278
21 Flaman, A. A. M., Thesis, Eindhoven, 1990, p. 117
22 Vainstein, B. K. 'Diffraction of X-rays by Chain Molecules', Elsevier, Amsterdam, 1966, p. 173
23 Samuels, R. J. 'Structured Polymer Properties', Wiley, New York, 1974, p. 63
24 Sawyer, L. C. and Jaffe, M. *J. Mater. Sci.* 1986, **21**, 1897
25 Weng, T., Hiltner, A. and Boer, E. *J. Mater. Sci.* 1986, **21**, 744
26 Barres, O., Jasse, B. and Noël, C. PPS-6, Nice, 1990
27 Nijman, G. Thesis, Twente, 1990, p. 41
28 Heynderickx, I. and Paridaans, F. *Polymer* 1993, **34**, 4068